

Realizing Parrondo's Paradox in Single-Qubit Quantum Walks via Local Phase-Induced Spatial Inhomogeneity

Ran-Yu Chang^{1,*}, Yun-Hsuan Chen², Gooi Zi Liang³, and Tsung-Wei Huang⁴

¹*Arete Honors Program, National Yang Ming Chiao Tung University, Hsinchu, Taiwan*

²*Concordia International School Shanghai, Shanghai, China*

³*Shanghai Highschool International Division, Shanghai, China and*

⁴*Department of Intelligent Computing and Big Data,*

Chung Yuan Christian University, Taoyuan, Taiwan

(Dated: August 27, 2025)

Parrondo's paradox describes a counterintuitive phenomenon where alternating between two individually losing games results in a winning expectation. While its classical origin relies on capital-dependent bias and noise-induced asymmetry, realizing a robust quantum version of the paradox has remained challenging, especially under the constraint of single-qubit coin systems. In this work, we demonstrate that a genuine quantum Parrondo effect can emerge in discrete-time quantum walks (DTQWs) by alternating two $SU(2)$ coin operators and introducing a localized phase shift at the origin. Through a series of numerical experiments, we show that this minimal model—without entanglement or high-dimensional coins—exhibits sustained positive drift only in the presence of spatial inhomogeneity. We analyze the role of phase angle, coin parameters, and game sequences, and identify optimal regions in which constructive interference enables paradoxical transport. Our findings validate recent theoretical claims that translational symmetry breaking is essential for overcoming interference-induced cancellation, thereby enabling directed quantum motion. This work opens new possibilities for realizing counterintuitive quantum dynamics using low-resource architectures, with potential applications in quantum control, energy harvesting, and coherence-assisted transport.

I. Introduction

Quantum walks, as quantum counterparts of classical random walks, constitute a fundamental framework in quantum algorithm design and quantum simulation. Since their inception by Aharonov et al. [1] and further formalization by Kempe [2], quantum walks have demonstrated superior spreading behavior due to quantum coherence and interference, achieving quadratic speed-up over classical diffusion. Their utility spans diverse domains, including quantum search algorithms [3], modeling quantum transport [4], and probing localization and topological phases in disordered systems [5, 6].

Parrondo's paradox, initially formulated by Parrondo and systematized by Harmer and Abbott [7], describes a phenomenon in which alternating between two individually losing games results in an expectation of overall victory. In classical implementations, Game A involves a biased coin with a negative expected value, whereas Game B employs a state-dependent bias modulated by a function of capital. Despite the individual negativity of both games, specific sequences such as AB or ABB can yield net gains [8–11]. This paradox is intimately linked with the statistical mechanics of Brownian ratchets[12].

The quantum version of Parrondo's paradox translates this concept into the framework of quantum stochastic processes, typically realized via discrete-time quantum walks (DTQWs). In this setting, classical biased coins are replaced by $SU(2)$ unitary operators acting on quantum coin

states, whose alternation emulates the interplay between losing strategies [13]. Foundational contributions by Flitney and Abbott [14] and Meyer [15] established that quantum interference could enable Parrondo-like behavior[16]. However, Flitney, Ng and Abbott [17] demonstrated that such effects are often transient and decay in the long-term limit. This led to a prevailing assumption that more intricate mechanisms were necessary to sustain the effect.

Consequently, several proposals emerged that extended beyond single-qubit architectures. These include history-dependent coin schemes [18], higher-dimensional coins such as qutrits [19], open quantum systems that incorporate decoherence [20], engineered noise [21], and asymmetric shift operators [22]. All of these designs share a foundational premise—that single-qubit implementations are insufficient for realizing a long-term quantum Parrondo effect. Rajendran and Benjamin [23] supported this by showing that stable Parrondo behavior can emerge with entangled two-coin initial states.

However, this perspective was nuanced by later developments. Chandrashekar and Banerjee [24] proposed a DTQW-based model showing that a properly constructed sequence of $SU(2)$ operations, even within a single-qubit coin system, can yield a measurable Parrondo effect. Their findings suggest that under carefully tuned conditions, the assumption of insufficiency in single-coin implementations may not be universally valid. Collectively, these studies highlight that the manifestation of the quantum Parrondo effect is not solely dictated by system dimensionality, but also by operator structure and interference dynamics [25].

A major experimental breakthrough was achieved by Jan et al. [26], who realized a quantum Parrondo walk on

* leo07010@gmail.com

an optical platform. By alternating two distinct SU(2) rotation operators, they simulated games A and B within a one-dimensional quantum walk. Their results provided empirical evidence of a persistent positive drift in the walker's mean position, consistent with theoretical predictions. This work has catalyzed subsequent experimental interest across multiple architectures, including trapped ions [27, 28], superconducting circuits [29], and photonic lattices [30].

Additionally, the simulation of quantum Parrondo's paradox has been refined through the introduction of an inhomogeneous coin structure [31]. Through the demonstration of a position-inhomogeneous quantum walk with an inhomogeneous coin, it is theoretically possible to achieve maximal coin-walker entanglement after any odd steps or large even steps asymptotically[31]. Their finding enables an efficient method for simulating physical systems that require high-dimensional entanglement with simpler coin structures. This result can thus be applied under the context of quantum Parrondo's paradox due to its property of achieving positive results under specific step and coin conditions.

Classical Parrondo's paradox, which illustrates how alternating two losing games can produce a winning expectation, has found real-world applications in a variety of fields. In genetics, it demonstrates that an autosomal allele can rise in frequency even with lower average fitness through antagonistic selection and epistatic interaction of alleles at two loci [32]. In population dynamics and evolutionary game theory, it explains how organisms can enhance survival by switching between disadvantageous behaviors, such as dormancy and reproduction [33, 34]. In ecological modeling, it has been used to describe how alternating nomadic and colonial strategies enable species to persist in degraded environments [33, 34]. In financial systems, the paradox underpins strategies where switching between individually losing assets or rules can lead to net gain [35–37]. In engineering, it contributes to the design of Brownian thermal engines and other systems where alternating between suboptimal states boosts overall efficiency [38]. In reliability theory, alternating between unreliable system configurations has been shown to improve long-term performance [39, 40]. These interdisciplinary applications underscore the counterintuitive but powerful insight that losing strategies can combine to win. With the rise of quantum technologies, we believe that quantum Parrondo games—leveraging quantum coherence and interference—will provide even more powerful and efficient solutions to simulate, optimize, and control such systems beyond classical limitations.

In this work, we systematically investigate the quantum Parrondo effect within single-coin discrete-time quantum walks by alternating SU(2) coin operators with varying phase parameters (α, β) , and by incorporating modulo conditions to emulate the classical structure of Game B. Our numerical simulations reveal that, within specific regions of the parameter space, alternating coin operations can induce a positive bias in the walker's mean position,

challenging the conventional view that a genuine quantum Parrondo effect cannot arise in single-coin systems. This study not only enriches the theoretical landscape of quantum Parrondo's paradox, but also opens new avenues for low-resource quantum control and algorithmic design[41].

In this work, we introduce a position-dependent phase-modified two-coin alternating quantum walk model. Specifically, coins A and B are two independent SU(2) operators that are alternated at each time step. However, whenever the walker is located at the origin position $x = 0$, we apply an additional phase factor $e^{i\phi}$ to the coin operation, regardless of whether coin A or B is being used.

This design is inspired by the inhomogeneous quantum walk framework proposed by Zhang et al. [42], where a local phase is applied at the origin to achieve maximal coin-walker entanglement. We are the first to incorporate this idea into the context of quantum Parrondo's games, constructing a novel “origin-phase-modified two-coin model” that bridges position-dependent interference with alternating losing strategies.

II. Methods

A. Simulation Platform

All simulations were performed using Qiskit 1.0 with the `AerSimulator` backend to numerically simulate the quantum walk evolution. The circuits were constructed and executed in Python 3.11.

B. Parrondo's Paradox

Mathematically, Parrondo's paradox arises from the nonlinear and asymmetric behavior of state-dependent stochastic processes. Consider two games, A and B, each involving biased coin tosses\cite{harmer1999losing}. Game A is set as a biased coin flip, where the player has a higher probability of losing, the probability of game A winning is defined as:

$$p_A = \frac{1}{2} - c, \quad \text{where } c > 0 \quad (1)$$

This results in the probability of winning in game A to be lower than the probability of losing, which makes game A a losing game overall.

Game B uses two coins based on capital modulo 3, the probability of winning for both coins of game B are defined as:

$$p_{B_1} = \frac{1}{10} - c \quad (\text{if capital } \bmod 3 \equiv 0) \quad (2)$$

$$p_{B_2} = \frac{3}{4} - c \quad (\text{otherwise}) \quad (3)$$

As shown, coin 1 of game B has a much lower chance of winning while coin 2 has a higher chance of winning.

In order to demonstrate that game B is a losing game,

we define a Markov chain with 3 states (capital mod 3). The transition matrix is defined as:

$$T = \begin{pmatrix} 0 & \frac{1}{10} & \frac{9}{10} \\ \frac{1}{4} & 0 & \frac{3}{4} \\ \frac{3}{4} & \frac{1}{4} & 0 \end{pmatrix} \quad (4)$$

Where state 0 uses coin 1 of game B, while state 1 and 2 uses coin 2 of game B. The stationary distribution is defined as:

$$\mathbf{d} = \left(\frac{5}{13}, \frac{2}{13}, \frac{6}{13} \right) \quad (5)$$

Expected winnings per state:

$$\mathbf{w} = \left(-\frac{4}{5}, \frac{1}{2}, \frac{1}{2} \right) \quad (6)$$

The overall expected value is:

$$\mathbf{d} \cdot \mathbf{w} = \frac{5}{13} \left(-\frac{4}{5} \right) + \frac{2}{13} \cdot \frac{1}{2} + \frac{6}{13} \cdot \frac{1}{2} = 0 \quad (7)$$

When the constant c is positive, this expectation becomes negative. Hence, game B is a losing game if played on its own.

C. Inhomogeneous Quantum Walk

We consider a discrete-time quantum walk with an inhomogeneous coin operator localized at the origin.

The SU(2) coin operator is defined as:

$$\hat{C}(\alpha, \beta, \gamma) = \begin{pmatrix} e^{i\alpha} \cos \beta & -e^{-i\gamma} \sin \beta \\ e^{i\gamma} \sin \beta & e^{-i\alpha} \cos \beta \end{pmatrix} \quad (8)$$

Let \hat{C}_A and \hat{C}_B denote the coin operators used in Game A and Game B, respectively. To introduce inhomogeneity, we modify the coin operator at position $x = 0$ by applying an additional phase shift ϕ :

$$\hat{C}_{A,B}(x) = \begin{cases} e^{i\phi} \cdot \hat{C}_{A,B} & \text{if } x = 0 \\ \hat{C}_{A,B} & \text{if } x \neq 0 \end{cases} \quad (9)$$

The initial state of the walker is:

$$|\Psi(0)\rangle = \frac{1}{\sqrt{2}}(|0\rangle - i|1\rangle) \otimes |0\rangle \quad (10)$$

At time t , the walker state evolves into:

$$|\Psi(t)\rangle = \sum_x [a_x(t)|0\rangle + b_x(t)|1\rangle] \otimes |x\rangle \quad (11)$$

Each time step of the quantum walk consists of:

- Coin operation:** Apply $\hat{C}_{A,B}(x)$ at each site x , with a localized phase at $x = 0$.

2. Conditional shift:

$$\hat{S} = \sum_x (|0\rangle \langle 0| \otimes |x+1\rangle \langle x| + |1\rangle \langle 1| \otimes |x-1\rangle \langle x|) \quad (12)$$

The total unitary operator per step is then given by:

$$\hat{U} = \hat{S} \cdot (\hat{C} \otimes \mathbb{I}) \quad (13)$$

D. Observables

We compute the following quantities for up to steps on a -site lattice:

- **Expected position (net gain indicator):**

$$\mathbb{E}[x] = \sum_x x \cdot P(x), \quad P(x) = |a_x|^2 + |b_x|^2 \quad (14)$$

Positive values of imply a winning game strategy, and negative values imply loss.

- **Winning probability difference (symmetry measure):**

$$\Delta P = P_{\text{right}} - P_{\text{left}} = \sum_{x>0} P(x) - \sum_{x<0} P(x) \quad (15)$$

This measures directional bias, indicating whether the walker prefers moving right (positive gain) or left (loss).

- **Coin-position entanglement entropy:**

$$\begin{aligned} \rho_c &= \text{Tr}_{\text{pos}}(|\Psi(t)\rangle \langle \Psi(t)|), \\ S(t) &= -\text{Tr}(\rho_c \log_2 \rho_c) \end{aligned} \quad (16)$$

This quantifies the entanglement between coin and position.

The reason we compute this observable is that in most quantum simulations of Parrondo's paradox, the coin-position entanglement is regarded as a signature of quantum interference. High entanglement is often associated with stronger manifestation of the paradoxical effect, as the walker's dynamics cannot be classically decomposed.

E. Simulation Details

Simulations are implemented in Python using double-precision complex numbers. The wavefunction is discretized on a 1D lattice. Coin parameters are fixed, and coin operators are applied according to specific game sequences. Unless otherwise stated, the phase at the origin is set to a default value.

III. Results and Discussion

We first investigate whether the introduction of a local phase at the origin can induce a quantum version of Parrondo's paradox using coin parameters previously shown to be non-parrondian individually. Specifically, we

adopt two SU(2) coin operators, \hat{C}_A and \hat{C}_B , inspired by Ref. [43], with parameters:

$$\hat{C}_A = R(\alpha_A, \beta_A, \gamma_A) = R(2.395, 0.513, 0.909),$$

$$\hat{C}_B = R(\alpha_B, \beta_B, \gamma_B) = R(2.611, 1.176, 2.313),$$

A. Quantum Parrondo Effect via Phase-Modified SU(2) Coins

Although Fig. 3 in Ref. [43] suggests that the ABB sequence yields a positive probability difference $P_R - P_L > 0$, our reproduced simulation reveals that this criterion alone is insufficient to confirm the existence of a true Parrondo effect. In particular, when we examine the expected position rather than the probability imbalance, we find that the ABB game continues to drift downward over time. This indicates that despite having more probability mass on the right, the overall motion remains biased in the losing direction.

This discrepancy arises from the fact that $P_R - P_L$ only captures the net difference in probability between the right and left sides of the lattice, without accounting for the spatial contribution of each position. For instance, a probability mass located at $x = 1$ contributes far less to the expected position than one at $x = 10$. As such, it is possible to have $P_R > P_L$ while the system is still moving left overall. This demonstrates that the expected position serves as a more physically meaningful and reliable indicator for detecting the presence of the Parrondo effect.

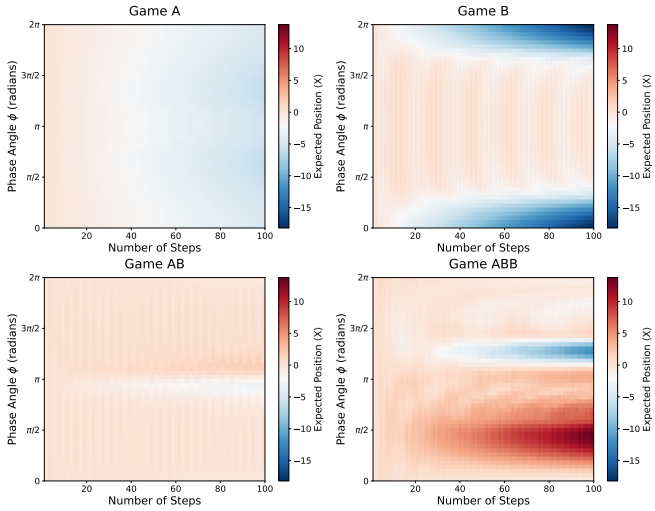


FIG. 1. Heatmaps of the expected position $\langle x \rangle$ as a function of the number of steps and the phase angle ϕ , for different coin sequences. Only the ABB sequence exhibits a consistent positive drift (red region) within a specific range of phase values.

Fig. 1 presents the expectation values after 100 steps for various values of the inhomogeneous phase parameter ϕ , applied locally at the origin. From the phase scan, we

observe that Game A consistently shows a clear downward trend across all phases, confirming it as a losing game. Game B exhibits strong negative drift in the intervals $\phi \in [0, \pi/4]$ and $[5\pi/4, 2\pi]$, and shows slow, oscillatory decay in the intermediate range $\phi \in [\pi/4, 5\pi/4]$. Game AB does not exhibit any significant drift across the entire range of ϕ , while Game ABB demonstrates a strong upward trend in the region $\phi \in [0, \pi]$. This observation confirms that the Parrondo effect only emerges in the presence of a locally inhomogeneous coin operator[44].

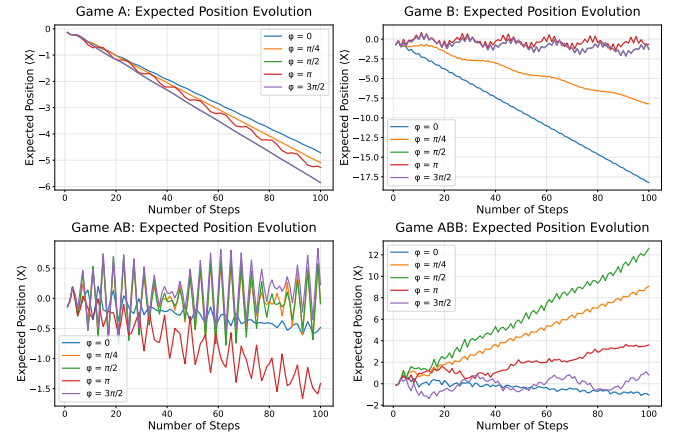


FIG. 2. Line plots of expected position $\langle x \rangle$ over time for five selected phase angles $\phi = 0, \pi/4, \pi/2, \pi, 3\pi/2$. Among all sequences, only Game ABB shows a strong positive drift at $\phi = \pi/2$.

To further examine the dynamical behavior, we select representative phase values $\phi = 0, \pi/4, \pi/2, \pi, 3\pi/2$, and plot the expected position over 100 time steps for each game sequence in Fig. 2. Game A exhibits steady decay regardless of the phase. Game B shows strong phase dependence: at $\phi = 0$ it drifts downward rapidly, while at $\phi = \pi$ the expectation remains nearly flat. Game AB remains near zero across all phases with only small oscillations. In contrast, Game ABB exhibits a distinct upward trend at $\phi = \pi/2$ and $\phi = \pi$, demonstrating the emergence of a net gain.

Interestingly, we also observe that in the individual games A and B, the curves corresponding to $\phi = \pi/2$ and $\phi = 3\pi/2$ almost perfectly overlap, suggesting an underlying symmetry in the quantum walk dynamics at these phases. However, this symmetry is broken in the composite games. While Game B alone shows slow decay at $\phi = \pi/2$, the ABB sequence under the same phase exhibits a strong positive drift. This striking contrast illustrates that the Parrondo effect does not arise from the individual games themselves, but rather from the interference accumulated through the sequence structure. The ordering of games, even when composed of individually losing components, can significantly reshape the interference landscape and yield constructive effects in the expected position.

Taken together, our results demonstrate that relying

solely on the probability difference $P_R - P_L$ may lead to misinterpretation of the system's behavior. The expected position provides a more faithful measure of the system's dynamical evolution and net bias. The structure of the sequence, the accumulation of interference history, and the presence of spatial asymmetry introduced by local phase shifts are all essential to realize a genuine quantum Parrondo effect.

B. Results II: Sensitivity to Initial Coin States

To further investigate the dynamical origin of the observed behavior, we examine the role of the initial coin state in shaping the quantum walk's expected position. In discrete-time quantum walks, the coin state determines the initial direction and symmetry of the interference pattern. While many studies focus on fixed coin states such as $\frac{1}{\sqrt{2}}(|0\rangle \pm i|1\rangle)$, the full parameter space of initial coin states introduces additional asymmetries that can significantly affect transport properties, especially in the presence of inhomogeneities.

To systematically explore this, we scan the full family of initial coin states of the form:

$$|\psi_c(0)\rangle = \cos \theta |0\rangle + e^{i\varphi} \sin \theta |1\rangle, \quad (17)$$

where $\theta \in [0, \pi]$ and $\varphi \in [0, 2\pi]$, while keeping the walker initialized at position $x = 0$.

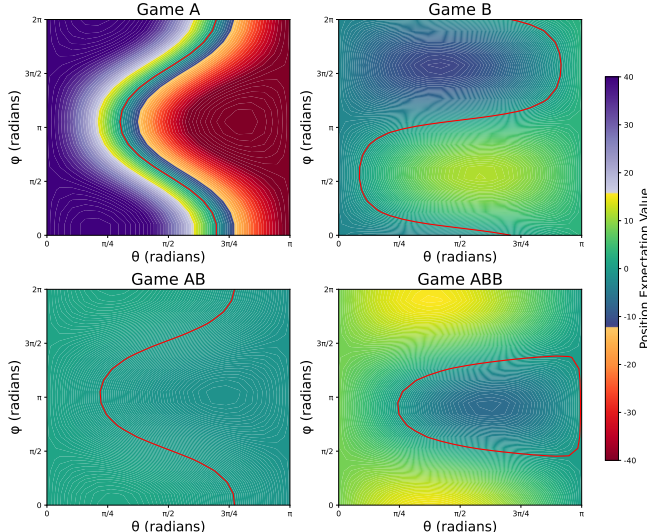


FIG. 3. Expected position after 100 steps as a function of initial coin state parameters θ and φ for different game sequences. Red contour line marks the zero-expectation boundary.

Fig. 3 shows the expected position after 100 steps across this two-dimensional parameter space for each game sequence. The red contour indicates the zero-mean line, separating regions of positive and negative expected position.

In Game A, a strong bias structure emerges, where the expectation value is highly sensitive to both θ and φ . A sharp transition from negative to positive expec-

tation occurs across a well-defined boundary, forming a smooth, diagonal contour. Game B also shows a structured, though more moderate, dependence on the initial coin state, with the boundary line (red contour) appearing distorted but continuous.

For Game AB, the expectation values are mostly centered around zero across the entire parameter space, indicating that the alternation of two losing games does not generate directional bias under any initial coin configuration. Game ABB, however, exhibits a strikingly different pattern. A large, closed region of positive expectation appears in the lower-left quadrant, bounded by the red contour line. This suggests that for certain initial coin states, the ABB game sequence leads to a strong forward drift, while others result in backward drift or stagnation.

These results highlight that the quantum Parrondo effect is not only sensitive to the sequence structure and local phase, but also to the symmetry and phase of the initial coin superposition. By tuning the coin state, one can effectively control the net drift direction, emphasizing the quantum walk's inherent sensitivity to initial conditions—a property with no classical counterpart.

C. Roles of Parameters in Coin Bias through β_A and β_B Scan with Fixed α and γ

In classical Parrondo games, the paradox arises when two individually losing games are combined in a periodic pattern to produce an overall winning outcome. To faithfully reproduce this logic in the quantum regime, we restrict our analysis to biased quantum coins whose behavior individually leads to a negative expected position. This corresponds to setting the coin angle $\beta \in [0^\circ, 90^\circ]$, where the quantum walker has a higher probability of moving in one direction, thereby mimicking a losing strategy.

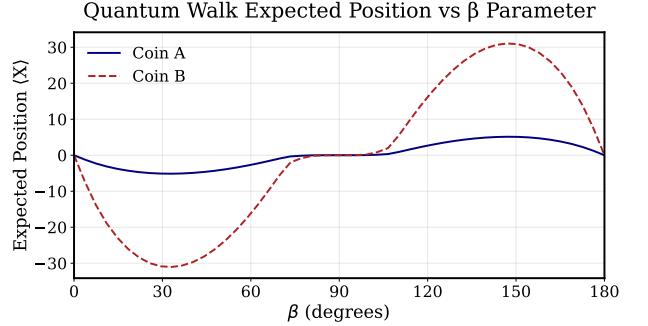


FIG. 4. Expected position $\langle x \rangle$ versus coin bias parameter β for single-coin quantum walks using Coin A (blue solid) and Coin B (red dashed). Only the range $\beta \in [0^\circ, 90^\circ]$ results in negative expected positions, consistent with losing behavior.

As shown in Fig. 4, both Coin A and Coin B produce negative drifts for $\beta < 90^\circ$, which we consider the "losing region." Beyond that point, the walker may exhibit symmetry or positive bias, which falls outside the classical intuition of Parrondo's paradox. Therefore, our focus is confined to the $[0^\circ, 90^\circ]$ region in all subsequent analyses.

We now explore how different combinations of coin

biases affect the overall transport behavior in multi-step games. Specifically, we examine the expected position of the walker in AB and ABB sequences as a function of the pair (β_A, β_B) , both ranging from 0° to 90° .

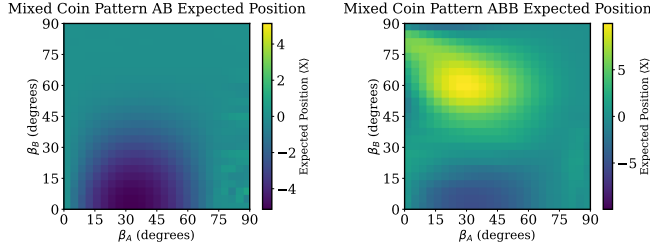


FIG. 5. Heatmaps of final expected position $\langle x \rangle$ after 100 steps for various combinations of coin parameters (β_A, β_B) in the AB (left) and ABB (right) sequences. While AB mostly results in near-zero or negative bias, the ABB sequence exhibits a clear region of positive drift in the upper-left region, indicating a robust quantum Parrondo effect.

Fig. 5 shows the parameter sweep results. For the AB sequence (left), the expected position remains centered around zero, suggesting the absence of long-term directional drift. In contrast, the ABB sequence (right) reveals a strong positive region when β_A is small and β_B lies in the range of 60° to 85° . This pattern is consistent with the quantum Parrondo effect: the individual coins are losing, but their strategic combination produces a winning outcome.

While the β parameter governs the overall bias of the coin (i.e., left vs. right movement), it is also important to understand how the coin's internal phase parameters— α and γ in the SU(2) coin definition—affect the interference dynamics and walker trajectory. Therefore, we extend our analysis by scanning α and γ independently while holding β fixed in the losing region.

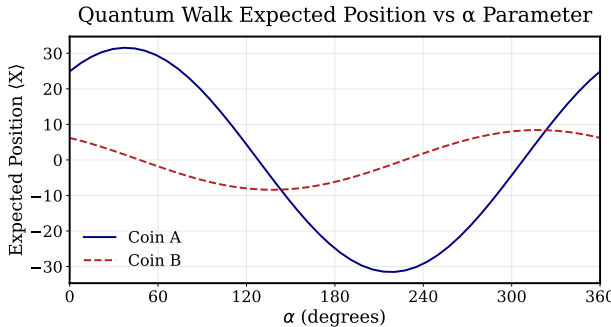


FIG. 6. Expected position $\langle x \rangle$ versus SU(2) parameter α , with fixed $\beta = 45^\circ$ and $\gamma = 0^\circ$. Coin A (blue) and Coin B (red dashed) display strong sinusoidal dependence on α .

From Figs. 6 and 7, we observe that the expectation value exhibits strong sinusoidal dependence on both α and γ , confirming their role in controlling the interference pattern. Interestingly, the oscillation amplitude is larger for Coin A, while Coin B responds more smoothly. This

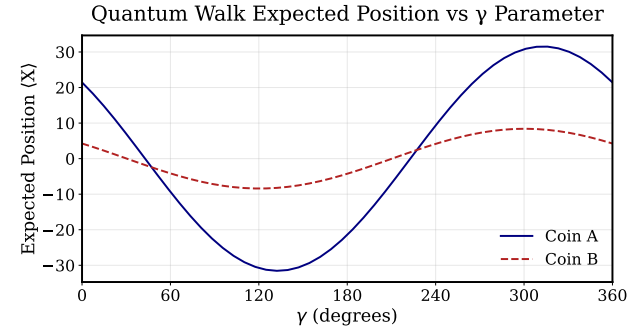


FIG. 7. Expected position $\langle x \rangle$ versus SU(2) parameter γ , with fixed $\beta = 45^\circ$ and $\alpha = 0^\circ$. Coin A and Coin B again exhibit distinct oscillatory behavior.

implies that α and γ introduce effective phase asymmetries that can amplify or suppress the walker's directional motion even when the bias β is fixed.

Finally, in Fig. 8 we scan the full (α, γ) parameter space to visualize the joint effect of these two internal parameters on the walk dynamics.

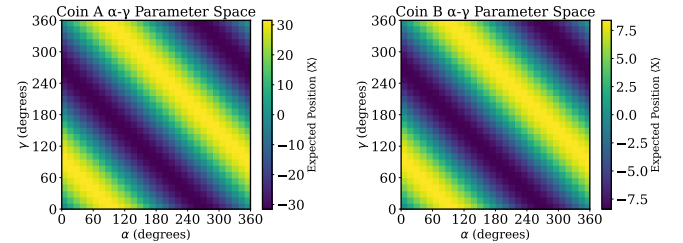


FIG. 8. Two-dimensional parameter space of α and γ for fixed $\beta = 45^\circ$. Coin A (left) and Coin B (right) show distinct interference patterns with diagonal symmetry, highlighting the entangled role of the SU(2) phase angles in shaping walker displacement.

The observed diagonal band structure reflects the combined phase interference induced by α and γ . Notably, Coin A produces higher contrast in expectation values across the diagonal, while Coin B exhibits smoother transitions. This further reinforces that α and γ can serve as fine-tuning parameters in controlling constructive or destructive interference within the quantum walk, particularly in scenarios where spatial inhomogeneity or game alternation is present.

Together, these findings demonstrate that while β controls directional bias, the SU(2) parameters α and γ encode the phase structure that governs interference. Their proper calibration enables precise control over walker dynamics and is essential to achieving robust Parrondo behavior in quantum systems.

IV. Conclusion

In this work, we have successfully demonstrated the realization of Parrondo's paradox within the framework of discrete-time quantum walks (DTQWs) using only a

single-qubit coin system. By carefully alternating two independently biased SU(2) coin operators and introducing a localized phase shift at the origin, we observed a genuine quantum Parrondo effect—namely, the emergence of a net positive drift in the walker’s average position, even though both underlying coin operations lead to negative expectation values when applied individually.

Our numerical simulations systematically validated this behavior across three experimental investigations. First, we showed that the ABB sequence with a position-dependent phase induces sustained directional transport, while the A, B, and AB sequences fail to produce net displacement. Second, we performed a full scan over the local phase angle ϕ and found that the paradoxical effect only emerges within a narrow region, with optimal behavior near $\phi = \pi/2$. Third, we explored the effect of the coin bias angles β_A and β_B , revealing a clear region in the $[0^\circ, 90^\circ]$ parameter space where the paradox persists, consistent with the classical requirement that both games must individually be losing.

These results provide strong support for recent theoretical claims [31, 42] that spatial inhomogeneity—specifically, the breaking of translational symmetry—plays a fundamental role in enabling the quantum Parrondo effect. The introduction of a local phase disrupts destructive interference and phase accumulation that otherwise neutralizes net transport in homogeneous walks. Our model thus establishes that highly counterintuitive behavior can be achieved using only minimal quantum resources: two single-qubit coins and a single-site phase operation.

Moreover, our findings highlight a distinct quantum

advantage. Even under highly unfavorable or classically losing strategies, quantum interference enables the suppression of non-productive paths and the amplification of constructive ones. The result is paradoxical success under conditions where classical analogues would consistently fail. The robustness of the observed effect, even when coin parameters are strongly asymmetric, further underscores the intrinsic power of quantum coherence in generating non-classical outcomes.

Importantly, the phase-controlled framework we propose is directly amenable to current experimental platforms such as quantum optics and superconducting circuits. Our results provide theoretical verification for simulating quantum Parrondo games on near-term hardware and offer a blueprint for experimental implementations that can probe foundational questions in quantum stochastic processes.

Looking forward, several exciting directions emerge from this work. Future investigations could extend this model to higher-dimensional lattices, two-particle or entangled-walker systems, and dynamic phase modulation strategies. Studying the impact of environmental decoherence and exploring the tradeoff between coherence and control precision will also be crucial for real-world implementations. Furthermore, the principles established here may be applicable in practical quantum technologies such as quantum energy harvesting, directed quantum transport, and coherence-assisted thermal machines. These avenues present rich opportunities for using engineered interference in low-resource quantum systems to achieve non-classical performance in computation, sensing, and control.

[1] Y. Aharonov, L. Davidovich, and N. Zagury, *Physical Review A* **48**, 1687 (1993).

[2] J. Kempe, *Contemporary Physics* **44**, 307 (2003).

[3] N. Shenvi, J. Kempe, and K. B. Whaley, *Physical Review A* **67**, 052307 (2003).

[4] H. B. Perets *et al.*, *Physical Review Letters* **100**, 170506 (2008).

[5] T. Kitagawa, M. S. Rudner, E. Berg, and E. Demler, *Physical Review A* **82**, 033429 (2010).

[6] T. Kitagawa, *Quantum Information Processing* **11**, 1107 (2012).

[7] G. P. Harmer and D. Abbott, *Statistical Science* **14**, 206 (1999).

[8] J. M. R. Parrondo, in *EEC HC&M Network Workshop on Complexity and Chaos* (1996).

[9] G. P. Harmer, D. Abbott, and P. G. Taylor, *Proceedings of the Royal Society A* **456**, 247 (2000).

[10] L. Dinis, *Europhysics Letters* **60**, 319 (2002).

[11] P. Reimann, *Physics Reports* **361**, 57 (2002).

[12] Q. Chen, Y. Wang, Y. Li, and J.-B. Xu, *Physics Letters A* **374**, 2830 (2010).

[13] D. A. Meyer, *Journal of Statistical Physics* **85**, 551 (1996).

[14] A. P. Flitney and D. Abbott, *Physica A: Statistical Mechanics and its Applications* **314**, 35 (2002).

[15] D. A. Meyer, *Physical Review Letters* **82**, 1052 (2002).

[16] A. P. Flitney, arXiv preprint (2012), arXiv:1209.2252 [quant-ph].

[17] A. Flitney, J. Ng, and D. Abbott, *Quantum parrondo’s games* (2002), arXiv:quant-ph/0201037.

[18] S. A. Bleiler and B. Khan, *Properly quantized history-dependent parrondo games* (2011), arXiv:1106.2774.

[19] J. Rajendran and S. C. Benjamin, *EPL (Europhysics Letters)* **122**, 40004 (2018).

[20] D. Ding, D.-L. Zhou, and Y.-D. Zhang, *Journal of Physics A: Mathematical and Theoretical* **45**, 125303 (2012).

[21] A. Romanelli, *Physical Review A* **80**, 042332 (2009).

[22] Y. Shikano and H. Katsura, *Physical Review E* **82**, 031122 (2010).

[23] J. Rajendran and S. C. Benjamin, *EPL (Europhysics Letters)* **90**, 10006 (2010).

[24] C. M. Chandrashekhar and S. Banerjee, *Parrondo’s game using a discrete-time quantum walk* (2011), arXiv:1101.3267.

[25] M. Jan, N. A. Khan, and G. Xianlong, *Territories of parrondo’s paradox and its relation with entanglement in quantum walks* (2022), arXiv:2006.16585 [quant-ph].

[26] M.-Y. Jan *et al.*, *Advanced Quantum Technologies* **3**, 1900127 (2020).

- [27] H. Schmitz, R. Matjeschk, C. Schneider, J. Glueckert, M. Enderlein, T. Huber, *et al.*, Physical Review Letters **103**, 090504 (2009).
- [28] F. Zähringer *et al.*, Physical Review Letters **104**, 100503 (2010).
- [29] E. Flurin *et al.*, Physical Review X **7**, 031023 (2017).
- [30] P. Xue *et al.*, Scientific Reports **5**, 12233 (2015).
- [31] V. Mittal and Y.-P. Huang, Phys. Rev. A **110**, 052440 (2024).
- [32] F. A. Reed, Genetics **176**, 1923 (2007), *pub* 2007 May 4.
- [33] K. H. Cheong, Z. X. Tan, and M. C. Jones, eLife **6**, e21673 (2017).
- [34] Z. X. Tan and K. H. Cheong, BMC Biology **19**, 1 (2021).
- [35] M. Stutzer, A simple parrondo paradox, <https://leeds-faculty.colorado.edu/stutzer/Papers/SimpleParrondoParadox.pdf> (2003), university of Colorado Boulder Working Paper.
- [36] W.-W. Xie, Y. Wang, and Q.-W. Wang, A study on the potential application of parrondo's paradox in industrial clusters, business strategy and public affairs, https://serialsjournals.com/abstract/25613-3-wei-wei_xie.pdf (2019), working Paper or Preprint.
- [37] R. Spurgin and M. Tamarkin, Journal of Behavioral Finance **6**, 15 (2005), https://doi.org/10.1207/s15427579jpfm0601_3.
- [38] J. M. R. Parrondo and B. J. de Cisneros, Applied Physics A **75**, 179 (2003), <https://arxiv.org/abs/cond-mat/0309053>.
- [39] A. Di Crescenzo, E. Di Nardo, and L. Riccicardi, Methodology and Computing in Applied Probability **9**, 497 (2007).
- [40] A. Di Crescenzo, ResearchGate preprint (2007), https://www.researchgate.net/publication/2125890_A_Parrondo_Paradox_in_Reliability_Theory.
- [41] G. Kadiri, Phys. Rev. A **110**, 022421 (2024).
- [42] R. Zhang, R. Yang, J. Guo, C.-W. Sun, J.-C. Duan, H. Zhou, Z. Xie, P. Xu, Y.-X. Gong, and S.-N. Zhu, Phys. Rev. A **105**, 042216 (2022).
- [43] M. Jan, Q. Wang, X. Xu, W. Pan, Z. Chen, Y. Han, C. Li, G. Guo, and D. Abbott, Advanced Quantum Technologies **3**, 1900127 (2020).
- [44] J. H. Bauer, Phys. Rev. E **111**, 064218 (2025).